RESEARCH ARTICLE

Optimization of novel nonaqueous hexanol-based monoethanolamine/methyl diethanolamine solvent for CO_2 absorption

Neslisah Ulus[1] | Shafeeq Ahmed Syed Ali[2] | Omar Khalifa[3] | Ozge Yuksel Orhan[1] | Ali Elkamel[4]

[1]Department of Chemical Engineering, Hacettepe University, Ankara, Turkey

[2]School of Engineering, Monash University, Subang Jaya, Malaysia

[3]Department of Chemical Engineering, Khalifa University of Science and Technology, Abu Dhabi, United Arab Emirates

[4]College of Engineering, University of Waterloo, Waterloo, Ontario, Canada

Correspondence
Ozge Yuksel Orhan, Department of Chemical Engineering, Hacettepe University, Ankara, 06800, Turkey.
Email: oyuksel@hacettepe.edu.tr

Summary

Chemical absorption of CO_2 into aqueous amine-based solvents is known as the most mature technology featuring high separation efficiencies and applicability of retrofitting. The high regeneration energy requirement of the process is a major drawback, and improvements in solvent design are required. This study investigated the CO_2 absorption and desorption performance of the nonaqueous monoethanolamine (MEA)/methyl diethanolamine (MDEA) blend experimentally using a stirred cell reactor. CO_2 loading, cyclic capacity loss, and initial absorption rate were measured for different solvent formulations and compared to single amines (MEA or MDEA). A mixture-process design and response surface methodology were employed to model and optimize the solvent formulation at different temperatures and pressures. The single-response optimization yielded 0.83 mol_{CO_2}/mol_{amine} (at 0% MEA and 303 K/0.5 barg) and 3.17e-5 $kmol/m^2 \cdot s$ (at 40% MEA and 310.67 K/0.5 barg) as optimal absorption capacity and rate of absorption, respectively. The multiresponse optimization was conducted using the composite desirability function yielding 0.653 mol_{CO_2}/mol_{amine} and 2.987e-5 $kmol/m^2 \cdot s$ ($D = 0.903$). The multiresponse optimization was also extended to include the impact of different initial settings and importance ratios between the absorption capacity and rate of absorption, in which the latter needed at least 1.6 higher importance level to influence the multiresponse optimization.

KEYWORDS
composite desirability, cyclic capacity, mixture design, multiresponse optimization, post-combustion capture, response surface methodology

1 | INTRODUCTION

With the rapid industrialization followed by automation in the past century, greenhouse gas (GHG) emissions are at an all-time high. The major consequence of which is global warming, and other environmental issues such as rising sea level, melting ice caps, rise in global temperature, floods, and droughts to name a few. Of the GHGs, carbon dioxide (CO_2) and methane (CH_4) are more detrimental owing to the volume of emissions and their long life span post emission in the atmosphere.[1] Hence, it becomes vital for device methods to reduce such emissions in the atmosphere actively.

Neslisah Ulus, Shafeeq Ahmed Syed Ali, and Omar Khalifa contributed equally to this study.

Energy supply and industrial sectors together account for over 77% of total emissions.[2] This is a consequence of the heavy dependence on fossil fuels in these sectors. Numerous studies have been conducted on the possible carbon capture technologies, including precombustion,[3,4] oxy-fuel combustion,[3,5,6] and post-combustion capture.[3,7] The latter is preferred due to its ease of adaptability into existing processes.[8] Furthermore, multiple techniques of post-combustion CO_2 capture are also being studied, namely absorption,[7,9] adsorption,[10,11] membrane-based separation,[12] biological separation,[13] and liquefaction or cryogenic separation.[14] Absorption methods, both physical and chemical, are the most promising and mature, and hence they are widely studied for industrial applications.[3]

Chemical absorption is suitable for low-pressure CO_2 capture, in which alkanolamines are the most prominent solvents. According to the number of nitrogen atoms and their connectivity, those solvents are categorized into primary, secondary, tertiary, sterically hindered, polyamines, and blended solvents.[8] Aqueous 30 wt% monoethanolamine (MEA) has been the benchmark solvent for chemical absorption of CO_2, while more attention is directed toward 40-wt% piperazine (PZ)/aminomethyl propanol with a 1:2 M ratio.[15] In general, primary amines have a low theoretical CO_2 absorption capacity (approximately 0.5 mol_{CO_2}/mol_{amine}) and have faster reaction rates with CO_2.[16] Secondary amines, such as diethanolamine (DEA), possess high reactivity rates and, consequently, can result in higher CO_2 absorption volumes. Yet, their choice is limited by the maximum loading capacity based on stoichiometry (0.5 mol_{CO_2}/mol_{amine}) and the energy intensity associated with the solvent regeneration during the stripping process,[17] similar to primary amines. Additionally, primary and secondary amines are more prone to solvent corrosiveness and solvent chemical instability. On the contrary, tertiary amines, such as methyl diethanolamine (MDEA), offer higher loading capacities (1.0 mol_{CO_2}/mol_{amine}) with a comparably less energy-intensive stripping process. Yet, tertiary amines exhibit slower kinetics than primary and secondary amines.[17] To overcome such shortcomings, blending amines could result in formulations with desirable properties. For example, combining primary or secondary amine with a tertiary amine would retain the individual positive traits while minimizing the negative characteristics, especially the MEA/MDEA blend.[8,18,19] An ASPEN optimization study on the Tenaga Nasional Berhad Research's pilot plant situated in Kajang, Selangor, was able to achieve a 300% reduction in energy penalty and heat duty cost when shifting to an MEA/MDEA mixture solvent from MEA solvent.[18]

Another aspect of solvent formulations is the cosolvent, which dictates the reaction chemistry and thermophysical properties. With typical aqueous-based solvents, the solvent regeneration step accounts for almost 70% of the total energy consumption.[20,21] This would impose high parasitic loads on power plants reaching 30% of the total energy being produced.[22,23] To mitigate this, either the absorption process should be modified[24] or the solvent should be innovated. Water could be supplemented or even replaced with organic cosolvents.[25,26] Such cosolvents can increase CO_2 solubility in tertiary amines as well as increase the absorption capacity.[27,28] These solvents are described as nonaqueous, water-free, or water-lean solvents, and they have been increasingly studied.[29,30]

Alkanolamine–alcohol blends are characterized by their high boiling point, low specific heat capacity, and low vaporization enthalpy. Such solvents can change phases upon their loading and separate into CO_2-lean and CO_2-rich phases,[31,32] where only the rich phase is sent into the stripper resulting in energy savings.[20,33] Li et al[33] evaluated the performances of various newly developed solvents for CO_2 absorption and their preliminary results showed that the use of alkanolamine–alcohol blends can reduce the regeneration energy requirement by almost 40% to 60%. Kim et al[20] studied the alkanolamine–alcohol mixtures of MEA and DEA with 1-heptanol, 1-octanol, and iso-octanol. It was found that the absorption capacity of nonaqueous MEA did not increase while increasing the amine concentration, whereas nonaqueous DEA solvents exhibited different capacities.

Studying such interactions imposed by nonaqueous solvents would be desired, especially with different amine concentrations. Design of experiment (DoE) is a powerful statistical approach toward modeling and conducting experimental engineering problems.[34] This is particularly helpful in shortening the experimental duration and resources instead of changing-one-factor-at-a-time methodology. Solvent formulations can be studied using mixture designs, in which the ratios of the components resemble the independent variables. Simplex-lattice and simplex-centroid designs are standard models for mixture components that are constrained to a certain sum (eg, ratios adding to 1).[35,36] Apart from the summation constraints, mixture designs have the same assumptions as factorial designs. Studying the solvent formulation can also be conducted at different levels of process variables, such as temperature and pressure using a mixture-process design.[37] Response surface methodology (RSM) is another subcategory of DoE, which can help in evaluating the response surface and determining the optimal response.[38] This is desirable especially in cases where

multiple factors affect the response or there are multiple responses to be considered. Within RSM, multiple designs can be used to model experiments and visualize the surface plots of the responses against the independent variables. These include factorial designs, central composite designs (CCD), Box-Behnken designs, among others.

Several studies have implemented DoEs such as RSM to optimize CO_2 absorption systems. Hemmati et al[39] studied CO_2 absorption using an intercooled post-combustion absorber column, where a rate-based model is used to predict industrial conditions. The data are then optimized using an RSM model to maximize CO_2 absorption and minimize cooling duty. Results showed that the optimum condition resulted in 3.3% increased CO_2 absorption. Song et al[40] used RSM to optimize a novel cryogenic CO_2 absorption system based on free-piston Stirling coolers. The experimental data were analyzed using multiple regression analyses and analysis of variance. The resulting mathematical models are utilized to derive the optimum conditions. Neethu et al[41] used a Box-Behnken design RSM to evaluate the performance of a microbial carbon capture cell. Various influential parameters such as nitrate concentration, photoperiod, and concentration of lipid extracted algae were evaluated. Results showed that the Box-Behnken design successfully optimized the process, making microbial carbon capture economical and efficient for scale-up. When it comes to aqueous amine solvents, Pashaei et al[42] used a CCD-RSM to model and optimize a PZ-based aqueous CO_2 absorption system. The optimization was conducted by considering various variables such as PZ concentration, liquid flow rate, CO_2 flow rate, and stirrer speed. The work by Nuchitprasittichai and Cremaschi[19] evaluated two of the prominent simulation-based optimization approaches for their aqueous amine-based CO_2 absorption system, a Box-Behnken design RSM and the more complex artificial neural networks (ANNs). Their results showed that the RSM design could model the system very well and yielded solutions with good accuracy. Setameteekul et al[43] employed a similar factorial RSM design to model and optimize the mass transfer coefficient in two systems with aqueous MEA and aqueous MEA/MDEA solvents, respectively. Anuar et al[44] used a CCD-RSM to model a novel hybrid solvent with 30-wt% MEA-tetrabutylphosponium methanesulfonate. Independent variables such as concentration, pressure, and temperature are evaluated, and the RSM-based model is evaluated against the experimental results. The experimental data reflected a percentage error between 0.6% and 2.11% when compared against the predicted results. Ali et al[45] evaluated the energy distribution and CO_2 removal efficiency of an aqueous MEA solvent system, which was then optimized using metamodels and RSM. The optimized configuration reduced heating and cooling demands by 62.77%, reduced total power consumption by 8.65%, and increased the separation performance by 4.46% in comparison with conventional processes. Yet, there is a scarcity of studies that employ DoE methods to optimize a mixture's composition for CO_2 absorption processes.

The primary objective of this study was to experimentally obtain the CO_2 absorption capacity, cyclic capacity loss (CL), and initial absorption rates of nonaqueous MEA/MDEA solvents using a stirred cell reactor. The solvent formulation was tested at different temperatures and pressures conditions. A mixture design was employed to account for the individuality of each component and any interactions that may occur. The optimization study is then conducted using RSM models, including single- and multiresponse optimization. Not only a novel solvent was investigated experimentally, but a collection of statistical tools was used to model and study such formulations, which can be adopted for future studies. Such a study exemplifies the importance of optimization analysis for more efficient use of energy.

2 | THEORY

Generally, the reactions between CO_2 and amine systems can be explained by two mechanisms. These are known as the zwitterion mechanism first introduced by Caplow[46,47] and the termolecular or (three-molecular) reaction mechanism first introduced by Crooks and Donellan.[48,49] The basic principle of the termolecular reaction mechanism is the assumption that an amine molecule reacts with both a CO_2 and a base molecule in a single step via the weakly bound intermediate product as given in Equation (1). Briefly, this mechanism involves the reaction of CO_2 with amine (here RNH_2) to form a carbamate (RNHCOO) by the deprotonation of the base.

$$CO_2 = RNH_2 \, B \rightleftarrows RNHCOO^- \, BH^+ \qquad (1)$$

The overall rate equation with respect to CO_2 (r_{CO_2}) is presented in Equation (2) which prevails when the dissolved CO_2 concentration is much less than those of others:

$$r_{CO_2} = k_o \, [CO_2] \qquad (2)$$

According to the modified termolecular reaction mechanism, Equation (3) is valid for the pseudo-first-order rate constants of MEA and linear alcohol (such as hexanol) (OH). Equation (4) is valid for hybrid systems consisting

of two reactants and a solvent, namely MEA, MDEA, and hexanol.[50,51]

The observed (or pseudo-first order) reaction rate constant (k_o) of all CO_2 reactions in hexanol is thus represented by the sum of the reaction rates given by the following equations.[52,53]

$$k_o = (k_{RNH_2}[RNH_2] + k_{OH}[OH])[RNH_2] \qquad (3)$$

where $[RNH_2]$ is the MEA concentration, $[OH]$ is the 1-hexanol concentration, and $[CO_2]$ is the CO_2 concentration in the liquid phase. k_{RNH_2} and k_{OH} are the experimental reaction constants. For the reaction of CO_2 with MEA/MDEA is given by:

$$k_o = (k_{RNH_2}[RNH_2] + k_{R_3N}[R_3N] + k_{OH}[OH])[RNH_2][R_3N] \qquad (4)$$

where $[R_3N]$ is the MDEA concentration.

3 | MATERIALS AND METHODS

3.1 | Chemicals

Industrially important alkanolamines, MEA and MDEA, were used to remove CO_2 in this study. The MEA (CAS no. 141-43-5) with a purity of ≥98% and MDEA (CAS no. 105-59-9) with a purity of ≥99% were purchased from Sigma-Aldrich (St. Louis, MO, USA). 1-Hexanol (CAS no. 111-27-3) with a purity of 98% was also purchased from Sigma-Aldrich. All these chemicals have been used as received without further purification. CO_2 and N_2 cylinders each with a 99.9% purity were supplied by Linde (Munich, Germany).

3.2 | Experimental apparatus and procedures

CO_2 absorption experiments were conducted in the bench-scale gas absorption apparatus shown schematically in Figure 1. The gas absorption system consists of a jacketed stirred cell reactor, CO_2 supply, N_2 supply, mass flow meter (MFM), mass flow controller (MFC), and a PID-controlled power control unit. The details of the apparatus and operating procedure of a gas–liquid stirred cell reactor can be found in our previous works.[54,55] Briefly, the stainless-steel reactor was 85 mm in diameter and had a 200-mL solvent reservoir. Both the liquid-phase and gas-phase impellers stirred at a constant speed of 500 rpm. Since the stirring speed is high, the mass
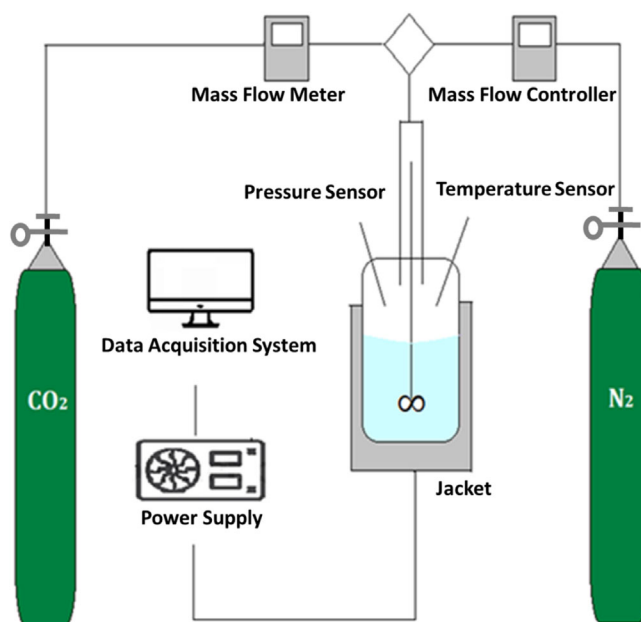

FIGURE 1 Schematic diagram of the experimental setup

transfer resistance is negligible. The temperature of the amine solution in the reactor was measured by the thermocouple thermometer mounted inside the bottom of the reactor with an accuracy of ±0.1%. The reactor pressure was measured by a pressure sensor mounted on the reactor with an accuracy of ±0.1%. The jacket, with ±0.2°C stability, was used for controlling the temperatures of both the CO_2 absorption and desorption experiments.

In absorption experiments, the flow rate of pure CO_2 entering the reactor was measured by the MFM (Model M-200SCCM-D/5M, Alicat Scientific Inc.). The flow rate of CO_2 leaving the reactor was controlled by the MFC (Model MC-200SCCM-D/5M, Alicat Scientific Inc.). The inlet and outlet CO_2 flow rates, temperature and pressure variation in the stirred reactor were recorded by a data logger every 10 s. The absorption process was continued until the inlet mass flow rate approached the outlet mass flow rate which means that the alkanolamine solvent reached equilibrium with CO_2. Then, the absorption curves (flow rate CO_2 [cm^3/min] vs time [s]) were plotted, and CO_2 absorption capacity (in mole) was determined through difference between flow rates as reported in our previous works.[56,57] The absorption capacity was presented in terms of CO_2 loading (mol_{CO_2}/mol_{amine}). Five consecutive absorption/desorption cycles were performed to verify the reusability and potential performance losses of alkanolamine solvents. Cyclic CL was developed in Equation (5). This equation describes the ratio of the mole difference of absorbed CO_2 in the first and fifth cycle to the absorbed CO_2 in the first absorption.

$$CL = \frac{n_{CO_{2_1}} - n_{CO_{2_5}}}{n_{CO_{2_1}}} \times 100\% \qquad (5)$$

A potential solvent system should have a high absorption capacity and also good durability. Therefore, CL results are crucial to imply the success of desorption performance. Minimum CL demonstrates higher desorption performance and better cycling stability.

The initial absorption rate (kmol/s) was calculated from the slopes of the CO_2 absorption curves at CO_2 loading ranges in 180 s where the initial absorption rate was highly accurate. CO_2 desorption experiments were carried out at 1.1 bar absolute N_2 pressure and 363 K.

3.3 | Design of experiments

A collection of statistical tools was used to design, model, and optimize the experiments, namely mixture-process design and RSM. The experimentation of the CO_2 capture using the novel solvent followed a combined mixture-process design, with a lattice design of two components (MEA and MDEA) and two process variables (temperature and pressure). A mixture design ought to measure, and possibly optimize, the amount of each constituent in a mixture on a specific set of responses. A given component can have an effect as per its sole existence in a mixture while exhibiting interactions with other components (positive or negative). As such, the goal of a mixture design is to map the surface of which can be described by a polynomial, with weights for individual components

and interactions if exist. Such mixture behavior might change in different settings, so it is desired to quantify a mixture design at different *process conditions*, which is the gist of a mixture-process design. In this study, a mixture of MEA and MDEA in hexanol ought to be modeled and optimized at different temperatures and CO_2 pressures. Hexanol concentration was fixed at 60%, in which five levels of concentrations were chosen for MEA and MDEA totaling 40%. Hence, the mixture design was only composed of two components. The process variables were varied at two levels (full factorial). The design can be seen as carrying out a five-level mixture design at each of the total factorial points of the process variables, or a two-level factorial of process variables at different points of the mixture spectrum (see Figure 2). As such, a total of 20 unique settings were carried out with replicas totaling 40 experiments. Additional 10 experiments were carried out at the center points of the process variables at each mixture composition to capture any unforeseen collinearity. The 40 experiments were used in the mixture-process design, while the total 50 experiments were used in a response surface methodology study, as the former does not allow three-level process variables. Accordingly, only MEA concentration was used along with the temperature and pressure in the RSM study as the MDEA concentration is a dependent variable ($x_{MDEA} = 0.4 - x_{MEA}$). The responses or independent variables were the absorption capacity and reaction rate. Minitab 19 was used to perform the statistical analysis and employment of the different models (mixture-process design and the RSM study). To guide the analysis and comparisons between

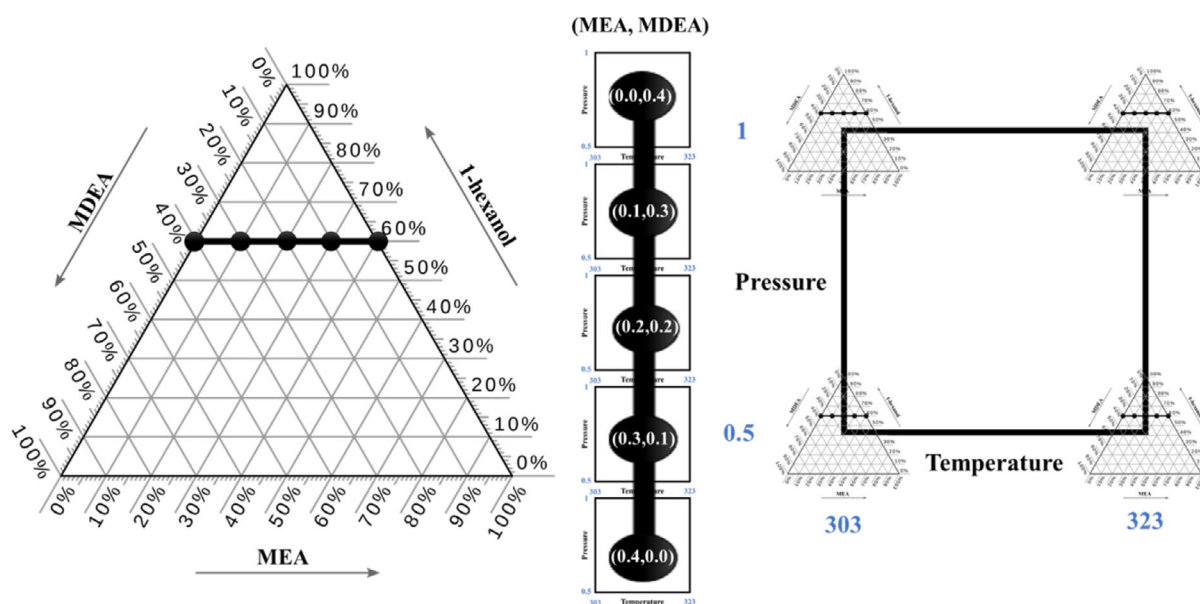**FIGURE 2** Visualization of the designs of experiments. Mixture design (left), process factorial design at each mixture point (center), and mixture design at each process factorial point (right). MDEA, methyl diethanolamine; MEA, monoethanolamine

the effect of other factors, four benchmark experiments were carried out at 313 K and 1 barg including aqueous MEA, aqueous MDEA, nonaqueous MEA, and nonaqueous MDEA at 30 wt% each.

3.4 | Optimization

The optimization of the MEA/MDEA mixture in hexanol was carried out through the mixture-process design and the RSM models. As such, the optimization of the mixture through two levels (mixture-process design) and three levels (RSM) was investigated. First, a single-response optimization study was conducted on both the mixture-process design and the RSM models. To fully cover the optimization spectrum, the initial condition of MEA was set at 0.4 for the reaction rate optimization, and the process conditions were varied over low (303 K, 0.5 barg), middle (313 K, 0.75 barg), and high (323 K, 1 barg) settings. Similarly, for the absorption capacity, MEA's concentration was set at 0.0 (initial condition) and varied over the same process variables settings as the reaction rate. The same trials were repeated for both mixture design optimization and RSM optimization.

The optimization of more than one response (two responses in this study) would require ranking their importance, or possibly treating all of them with the same weight. The composite desirability is the measure that describes how good is the overall optimization concerning all the responses, reflected by the maximum achievable values for each response. Hence, the higher the composite desirability, the closer the values are from the optima (if responses were treated individually). The individual desirability function (d_i) for maximizing a response is calculated using the following equation[58]:

$$d_i(y_i) = \begin{cases} 0, & y_i < L_i \\ \left(\frac{y_i - L_i}{T_i - L_i}\right)^{w_i}, & L_i \leq y_i \leq T_i \\ 1, & T_i < y_i \end{cases} \quad (6)$$

where y_i is the predicted response, L_i is the lower limit, T_i is the target value, and w_i is the importance of response i. The composite desirability (D) is calculated through the following equation (Minitab):

$$D = \left(\prod(d_i^{w_i})\right)^{\frac{1}{W}} \quad (7)$$

where, W is the summation of w_i.

The optimization results are also sensitive to the initial points, especially when dealing with nonlinear models. Also, setting targets and minimum values would

ultimately change the optima if not abating them at all. As such, multiple optimization settings ought to be investigated, which included initial values at 0 (minimum) and 0.4 (maximum) for MEA at low (303 K, 0.5 barg), medium (313 K, 0.75 barg), and high (323 K, 1 barg) process conditions. Those settings were tested at 1:1 and 1:2 importance levels for the absorption capacity to the reaction rate, while 1:4 and 1:8 were also tested for middle process variable settings at low and high MEA concentrations (see Table 3). The target for both responses was set as 0.75 of their respective ranges. As seen in the results and discussion section of the opposing trends of both the responses, an overlap of the optima of both responses does not exist, in which a trade-off is necessary. For the mixture-process design, the optimization would be limited to the boundaries of the process variables (minimum or maximum) as only two levels exist. This might oversee an optimum in between. Thus, the multiresponse optimization is better suited using the RSM model as per the availability of the center points of the process variables (third level). All optimization studies were conducted using the Response Optimizer option in Minitab 19.

4 | RESULTS AND DISCUSSION

4.1 | Experimental results

Stirred cell reactor is one of the widely used gas–liquid contactors for determining the performance of CO_2 separation. In this study, to determine the effects of amine concentration, temperature and CO_2 pressure on the absorption capacity, cyclic CL, and initial rate of absorption; 50 runs of CO_2 absorption experiments were performed using a stirred cell gas–liquid contact reactor under different CO_2 partial pressures (0.5, 0.75, and 1.0 barg) and operating temperature range of 303 to 323 K. The experimental results for single- and blended-amines were given in Table 1. For a typical run, 30 mL of fresh nonaqueous alkanolamine solution of the desired concentration was placed in the reactor. The total amine concentration was kept fixed at 40 wt%. Then, the reactor was heated to the desired temperature, and pure CO_2 was fed into the stirred cell reactor until the desired pressure was reached.

The results showed that amine concentration is the most important parameter in the chemical absorption of CO_2. The loading capacity of CO_2 absorption was found to increase with increasing MDEA. This was confirmed by the benchmark experiments, in which both aqueous and nonaqueous solutions of MDEA surpassed the capacity of their MEA counterparts (Figure 3). Yet, the absorption capacities for the aqueous solutions were slightly higher than those of the nonaqueous, which possibly

TABLE 1 Summary of results of all experiments

No.	MEA (conc. %)	MDEA (conc. %)	Temperature (K)	CO_2 pressure (barg)	CO_2 loading (mol_{CO_2}/mol_{amine})	Capacity loss after fifth cycle (%)	Rate of absorption ($kmol/m^2 \cdot s$) $\times$ (10^5)
1	40	0	303	0.5	0.39	25.23	3.114
2	20	20	303	0.5	0.55	18.97	3.078
3	0	40	303	0.5	0.87	19.10	2.646
4	30	10	303	0.5	0.45	26.00	3.092
5	10	30	303	0.5	0.67	25.32	2.997
6	40	0	303	0.5	0.37	22.45	3.117
7	20	20	303	0.5	0.51	19.75	3.081
8	0	40	303	0.5	0.84	18.35	2.708
9	30	10	303	0.5	0.45	25.65	3.094
10	10	30	303	0.5	0.65	23.09	3.004
11	40	0	323	0.5	0.23	33.31	3.124
12	20	20	323	0.5	0.28	23.02	3.081
13	0	40	323	0.5	0.55	21.11	3.121
14	30	10	323	0.5	0.33	33.31	3.095
15	10	30	323	0.5	0.39	30.14	3.008
16	40	0	323	0.5	0.22	30.14	3.128
17	20	20	323	0.5	0.25	27.23	3.082
18	0	40	323	0.5	0.54	20.16	3.124
19	30	10	323	0.5	0.32	29.50	3.096
20	10	30	323	0.5	0.38	29.50	3.021
21	40	0	303	1.0	0.32	18.79	3.128
22	20	20	303	1.0	0.46	23.37	3.085
23	0	40	303	1.0	0.68	18.65	2.867
24	30	10	303	1.0	0.39	22.84	3.099
25	10	30	303	1.0	0.54	24.59	3.023
26	40	0	303	1.0	0.30	15.55	3.132
27	20	20	303	1.0	0.44	24.09	3.086
28	0	40	303	1.0	0.66	24.67	2.873
29	30	10	303	1.0	0.37	23.45	3.103
30	10	30	303	1.0	0.56	23.87	3.054
31	40	0	323	1.0	0.21	26.56	3.139
32	20	20	323	1.0	0.25	18.85	3.087
33	0	40	323	1.0	0.44	20.63	3.134
34	30	10	323	1.0	0.25	16.28	3.106
35	10	30	323	1.0	0.32	25.23	3.062
36	40	0	323	1.0	0.21	25.79	3.146
37	20	20	323	1.0	0.23	21.11	3.089
38	0	40	323	1.0	0.47	23.17	3.143
39	30	10	323	1.0	0.24	17.75	3.107
40	10	30	323	1.0	0.29	25.49	3.072
41	40	0	313	0.75	0.31	26.24	3.123
42	20	20	313	0.75	0.38	21.67	3.107

TABLE 1   (Continued)

No.	MEA (conc. %)	MDEA (conc. %)	Temperature (K)	CO$_2$ pressure (barg)	CO$_2$ loading (mol$_{CO_2}$/mol$_{amine}$)	Capacity loss after fifth cycle (%)	Rate of absorption (kmol/m^2·s) × (10^5)
43	30	10	313	0.75	0.35	20.91	3.114
44	10	30	313	0.75	0.44	22.41	3.100
45	0	40	313	0.75	0.58	16.83	3.091
46	40	0	313	0.75	0.30	26.97	3.129
47	20	20	313	0.75	0.36	18.02	3.109
48	30	10	313	0.75	0.32	18.47	3.115
49	10	30	313	0.75	0.42	23.39	3.101
50	0	40	313	0.75	0.57	16.28	3.099

Abbreviations: MDEA, methyl diethanolamine; MEA, monoethanolamine.
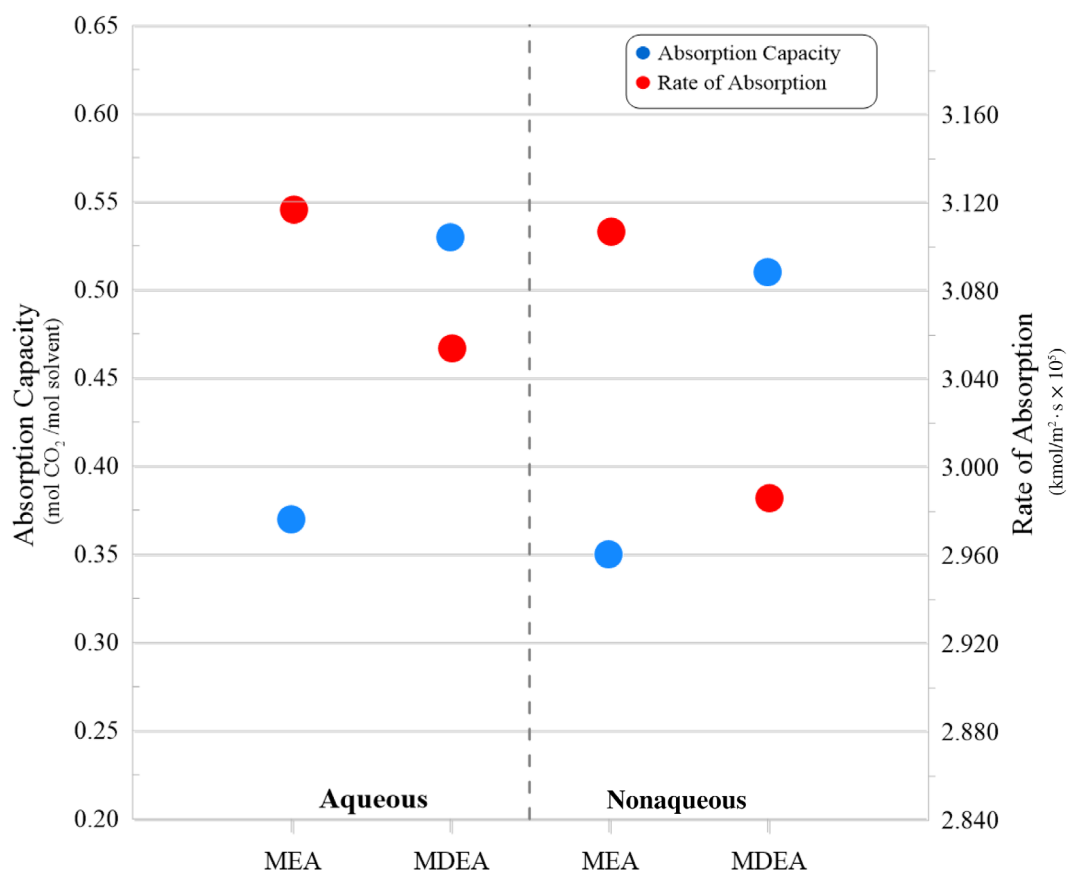

FIGURE 3   Absorption capacity and reaction rate of the benchmark experiments. All solutions are at 30 wt% (313 K and 1 barg)

indicates the inhibition of the reaction or the promotion of different mechanisms. Barzagli et al reported that the higher loading values were obtained in an aqueous solution, thanks to the formation of both carbamate and bicarbonate. While in the organic solvent, only the carbamate formation can occur and the amine loading was close to the theoretical value of 0.5.[59] The reaction rate for MEA was higher than that of MDEA for both aqueous and nonaqueous solutions, which is expected as per the governing mechanism for each amine. There was a drop in the reaction rate for both amines in nonaqueous solutions compared to their aqueous counterparts, yet a more pronounced effect was observed for MDEA, which signifies the importance of water in facilitating CO$_2$ absorption. This drop could also be attributed to the lower basicity of hexanol compared to the water. Also, a blend

of MEA/MDEA (20%/20%) has shown similar trends in capacity and reaction rate when experimented in aqueous and nonaqueous media. The capacity was 0.37 and 0.43, while the reaction rate was 3.108e-5 and 3.109e-5 kmol/m^2·s, for aqueous and nonaqueous solvents, respectively. Looking into the main effect plots of the CL at the fifth cycle as a ratio of the first cycle's capacity (Supporting Information S1), the high temperature and low pressure showed the highest CL, while no clear trend was observed for different MEA concentrations. Represented as a ratio, all values of CLs in the main effects plot ranged between 20% and 26%. This is primarily because the main effects plot ignores interactions between factors. Also, if the CL is studied without considering the capacity itself, this would entail that each setting (a given blend at a specific temperature and pressure) yields the same amount of CL, which is not the case. As such, the conclusion taken from such a plot should be conservative.

To get a sense of how the capacity of the studied solvent compares to other solvents in the literature, a summary of absorption capacity results from the literature for aqueous and nonaqueous amine systems is provided in Table 2.

4.2 | Mixture-process design

Equations (8) and (9) show the models obtained for the absorption capacity and reaction rate with R^2 values of 97.36% and 90.80%, respectively.

$$
\begin{aligned}
\text{Absorption Capacity} & \left(\frac{\text{mol}_{CO2}}{\text{mol}_{\text{solvent}}} \right) \\
= {} & 12.6806 x_{\text{MDEA}} + 5.2806 x_{\text{MEA}} + 6.7518 x_{\text{MDEA}} x_{\text{MEA}} \\
& - 0.0339 x_{\text{MDEA}} T - 0.0139 x_{\text{MEA}} T - 0.0304 x_{\text{MDEA}} x_{\text{MEA}} T \\
& - 0.6732 x_{\text{MDEA}} P - 0.2532 x_{\text{MEA}} P + 1.2143 x_{\text{MDEA}} x_{\text{MEA}} P
\end{aligned}
$$

(8)

$$
\begin{aligned}
\text{Reaction Rate} & \left(\frac{\text{kmol}}{\text{m}^2.\text{s}} \right) = -5.5950 x_{\text{MDEA}} + 6.2316 x_{\text{MEA}} \\
& + 81.8783 x_{\text{MDEA}} x_{\text{MEA}} \\
& + 0.0402 x_{\text{MDEA}} T + 0.0048 x_{\text{MEA}} T \\
& - 0.2526 x_{\text{MDEA}} x_{\text{MEA}} T \\
& + 0.5181 x_{\text{MDEA}} P + 0.0906 x_{\text{MEA}} P \\
& - 2.4679 x_{\text{MDEA}} x_{\text{MEA}} P
\end{aligned}
$$

(9)

The residual plots of both models can be found in the Supporting Information S1. As expected, the effect of MDEA on the absorption capacity is positive and higher than that of MEA, which is attributed to the reaction mechanism of each amine. The interaction between both amines appeared to lie between MEA and MDEA, which indicates that an MEA-based solvent would yield a higher

capacity when blending it with MDEA and vice versa. The temperature and pressure adversely affected the capacity with respect to both MEA and MDEA. Using only two levels of both process variables, low temperatures and pressures are preferred for high capacity, which is expected for exothermic chemical absorption reactions of CO_2.[8] The third order terms, $x_{\text{MDEA}} x_{\text{MEA}} T$ and $x_{\text{MDEA}} x_{\text{MEA}} P$, are the least significant, whereas interactions between process variables were omitted as per their insignificance. Overall, as inferred from the response trace plot Figure 4, it is desired to increase the MDEA's concentration while reducing MEA's to achieve the highest absorption capacity. This trend is consistent at different conditions of process variables.

The reaction rate increases with MEA's concentration while drops with MDEA. Primary amines, such as MEA, are known to have fast kinetics, while tertiary amines, including MDEA, are known to have slow reaction rates (approximately three to four orders less than primary amines).[74] Yet, the interaction between the concentration of MEA and MDEA appears to be significant and comparable to single effects of MEA and MDEA. For the process variables, increasing the temperature and pressures resulted in a nonlinear increase of the reaction rate, with respect to the interaction with MEA's and MDEA's concentrations. The overall effect of process variables can be seen in the response trace plot in Figure 5. The low-temperature settings, that is, 303 K/0.5 barg and 303 K/1 barg, exhibit the same behavior. Generally, the higher the concentration of MEA the higher is the rate, whereas the opposite trend is observed for MDEA. Yet, as of the interaction, there is a maximum rate at 0.3/0.1 (MEA/MDEA) for both low-temperature settings. For the high-temperature settings, the reaction rate has a minimum at the point 0.1/0.3 (MEA/MDEA) at 0.5 barg, while it reaches a minimum at 0.2/0.2 (MEA/MDEA) at 1 barg. This exemplifies that the temperature's effect is more pronounced than the pressure. However, at the high T/high P setting, the reaction rate seems to be unaffected by the type of component; the increase of MEA or MDEA decreases the rate up to 0.2, which increases afterward. Such findings exemplify the interaction of temperature and pressure.

4.3 | Response surface methodology

To further investigate the effect of the process variables on the responses with respect to the concentration of the components, an RSM study was conducted using the same points of the mixture-process design in addition to five replicated center points (10 points). The models along with the residual plots are shown in Supporting

TABLE 2 Comparison of absorption capacities of various CO_2 capture agents

Amine	Solvent	Concentration	Temperature (K)	CO_2 pressure (barg)	CO_2 loading (mol_{CO_2}/mol_{amine})
MEA	Water	30 (wt%)	313.15	1	0.58[60] 0.4-0.6[61]
MEA	Water	30 (wt%)	313.15	1	0.3[62]0.44[63]
MEA	Water	30 (wt%)	303.15	1	0.41[64]
MEA	Water	30 (wt%)	303.15	1	0.50[65]
MEA	N-methylformamide	30 (wt%)	303.15	1	0.49[65]
MEA	Diethylene glycol monomethyl ether	30 (wt%)	303.15	1	0.48[65]
MEA	Ethylene glycol/1-propanol	30 (wt%)	303.15	1	0.47[65]
DEA	Water	30 (wt%)	313.15	1	0.53[60] 0.49[66]
DEA	Diethylene glycol monomethyl ether	30 (wt%)	313.15	1	0.52[59]
MDEA	Water	30 (wt%)	313.15	1	0.52[60] 0.4-0.6[61]
DEEA	Water	30 (wt%)	313.15	1	0.9[60]
EMEA	Water	40 (wt%)	313.15	1	0.64[67]
EMEA	Ethanol	40 (wt%)	313.15	1	0.51[67]
AMP	Water	30 (wt%)	313.15	1	0.8[60] 0.78[62]
AMP	Diethylene glycol monomethyl ether	30 (wt%)	313.15	1	0.49[59]
AMP/MEA	Water	18 (wt%) MEA 12 (wt%) AMP	303.15	-	0.63[64]
AMP/MEA	Water	12 (wt%) MEA 18 (wt%) AMP	303.15	-	0.72[64]
AMP/MEA	Water	1 M MEA 3 M AMP	313	1.19	0.84[68]
AMP/MDEA	EG/methanol	2:1 AMP/MDEA	293.15	1	0.70[69]
AMP/DEA	EG/methanol	2:1 AMP/DEA	293.15	1	0.65[69]
AMP/DEA	1-Propanol	2:1 AMP/DEA	293.15	1	0.70[69]
PZ/DETA	Water	4 M PZ 4 M DETA	323.15	1	1.02[70]
PZ/DETA	DEG	4 M PZ 4 M DETA	303.15	1	0.92[70]
MEA/ MDEA/PZ	Water	3 M MEA 2.5 M MDEA 0.5 M PZ	313.15	1	0.39[63]
MEA/ MDEA/PZ	Water	3 M MEA 2 M MDEA 1 M PZ	313.15	1	0.44[63]
MEA/ MDEA/PZ	Water	3 M MEA 1.5 M MDEA 1.5 M PZ	313.15	1	0.46[63]
MEA/MDEA	Water	3:1 MEA/MDEA	303.15	1	0.70[71]
MEA/MDEA	Water	3:1 MEA/MDEA	313.15	1	0.67[71]

(Continues)

TABLE 2 (Continued)

Amine	Solvent	Concentration	Temperature (K)	CO_2 pressure (barg)	CO_2 loading (mol_{CO_2}/mol_{amine})
MEA/MDEA	Water	1:3 MEA/MDEA	303.15	1	0.72[71]
MEA/MDEA	Water	1:3 MEA/MDEA	313.15	1	0.69[71]
PZ	Water	30 (wt%)	313.15	1	0.81[60]
DEAB	Water	2 M	298		0.58[72]
Octylamine	Water	40 (wt%)	293.15	1	0.95[73]
Octylamine	Heptane	40 (wt%)	293.15	1	0.80[73]

Abbreviations: AMP, aminomethyl propanol; DEA, diethanolamine; DEAB, 4-diethylamino-2-butanol; DEEA, N,N-diethylethanolamine; DEG, diethylene glycol; EG, ethylene glycol; EMEA, N-ethylmonoethanolamine; MDEA, methyl diethanolamine; MEA, monoethanolamine; PZ, piperazine.
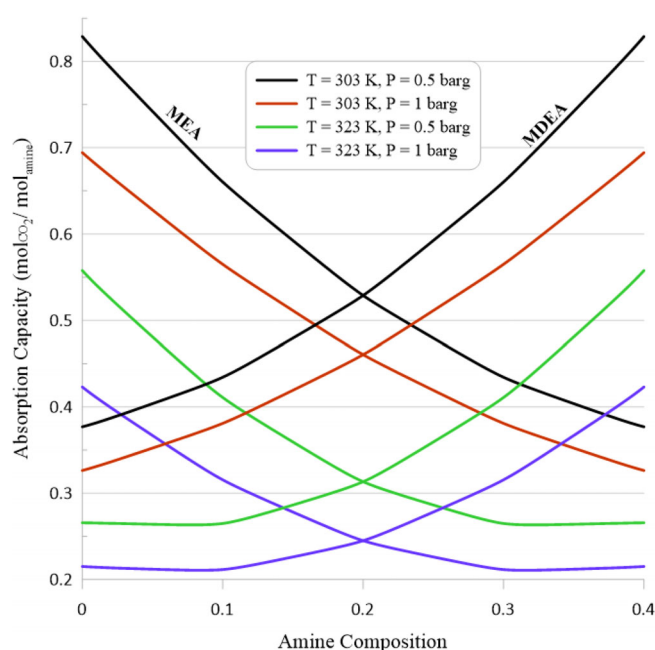
FIGURE 4 Response trace plot for the absorption capacity at different conditions and amine concentrations. MDEA, methyl diethanolamine; MEA, monoethanolamine

Information S2. The RSM results were found to be complimenting the mixture analysis, with each model providing a similar trend as observed before. In the case of absorption capacity, MEA concentration, process temperature, and pressure, all adversely impacted the model. The higher order interaction terms were omitted owing to their insignificance. As observed from the main effects plot (Figure 6), the absorption capacity was found to be the highest at low temperatures and pressures. The addition of center points helped to show that the drop in absorption capacity is not linear with respect to the process conditions. Yet, it should be noted that main effects graphs overlook the interactions between factors. Also, from the contour plot (Figure 7), it can be observed that

any increment in MEA concentration was always supplemented by a substantial decrease in the absorption capacity at high temperatures and high pressures. This shows that the model correctly predicts the general effect of the amines' concentration on the absorption capacity, in which adding more MEA at the expense of MDEA reduces the capacity of the amine blend.

For the case of rate of absorption, positive impacts are observed from MEA concentration, process temperature, and pressure. Here as well the higher order interaction terms were omitted owing to their insignificance. The main effects plot is shown in Figure 8. A maximum rate of absorption was observed at the center point, in the case of both temperature and pressure. To either extreme of the process parameter, the rate of absorption was found to decrease. Yet, the model still performed better than lower extremes at higher temperatures and pressures. Studying the contour plots, the rate of absorption is found to increase with increments in MEA concentration. Unlike absorption capacity, the rate of absorption was found to be high at higher temperatures and pressures. An exception in the aforementioned trend was shown for a mixture with an equal concentration of MEA and MDEA. A peak was observed in the contour graph (Figure 9), at the average temperature and pressure.

Four confirmatory experiments were conducted at midpoints to affirm the nonlinearity of the model as it appears in Table 3. The results for the absorption capacity (CO_2 loading) and reaction rate were in good agreement with the predictions from the respective models.

4.4 | Single-response optimization

Optimization of single responses was conducted using both models. Starting at different process conditions'
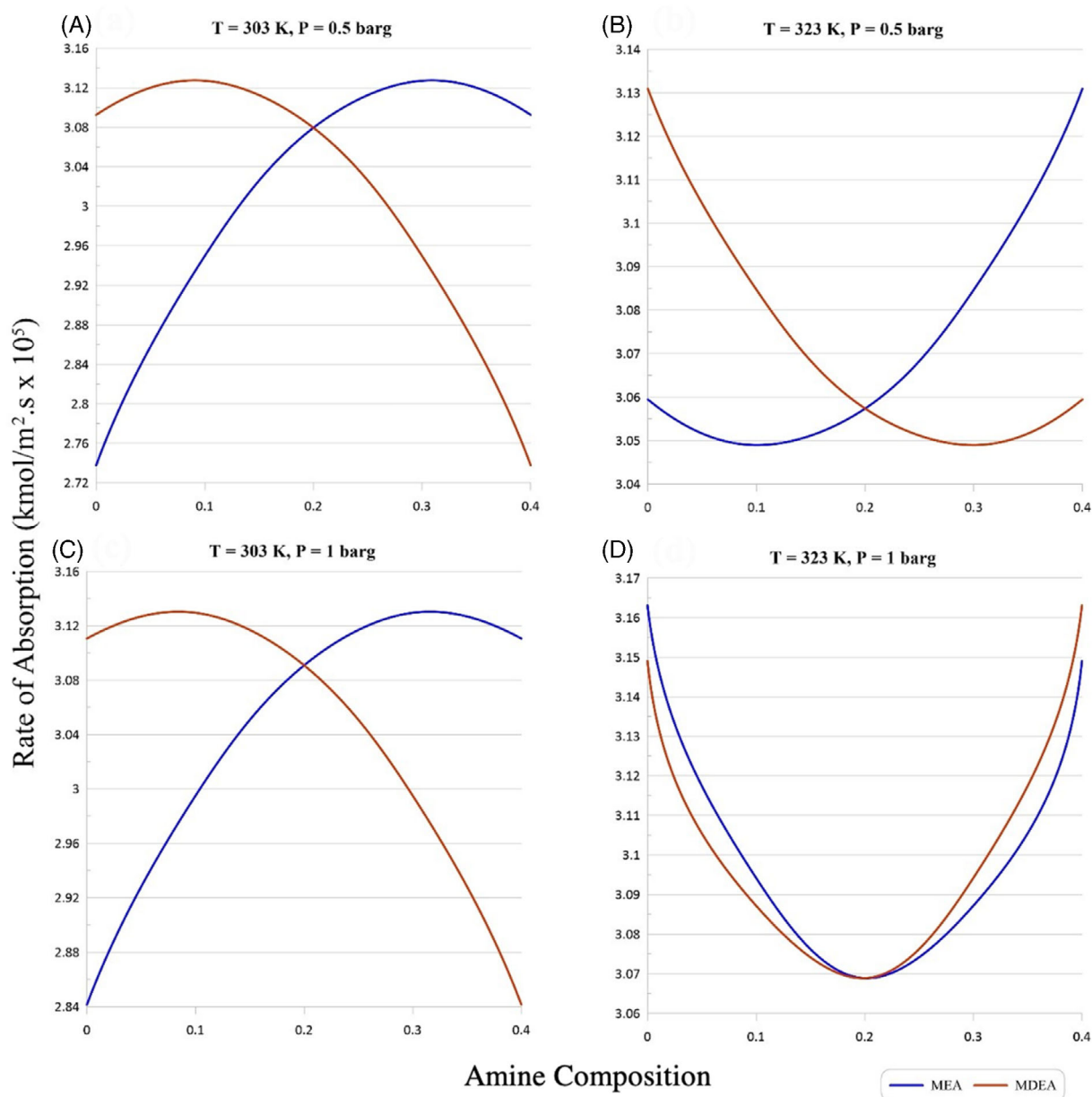
FIGURE 5 Response trace plots for the rate of absorption at A, low temperature and pressure; B, high temperature and low pressure; C, low temperature and high pressure; and D, high temperature and pressure

initial settings, the highest absorption capacity was 0.83 using both the mixture-process and the RSM models. This was achieved at 0.0/0.4 MEA/MDEA and 303 K/0.5 barg conditions. This is an expected result given that the higher the concentration of MDEA the higher the absorption capacity. Higher capacity is also achieved at lower process levels, which can be seen visually in Figure 4.

For the reaction rate, the mixture-process model predicted an optimum at 3.15e-5 kmol/m^2·s at 0.0/0.4 MEA/MDEA and 323 K/1 barg, while the RSM optimization yielded an optimum at 3.17e-5 kmol/m^2·s at 0.4/0.0

MEA/MDEA and 310.67 K/0.5 barg conditions. As only two levels of the process conditions exist for the mixture-process model, the optimum is found at the boundary of those conditions. Yet, it was not expected to have the optimum reaction rate at 0 concentration of MEA at the expense of MDEA, given that MEA is known to have faster kinetics than MDEA. In the RSM optimization, a higher reaction rate was achieved at the maximum concentration of MEA. Two factors might influence this observation. First, the initial setting for the mixture-process model that yielded this result was set at the same condition, that is, 0.0/0.4 MEA/MDEA and 323 K/1 barg.
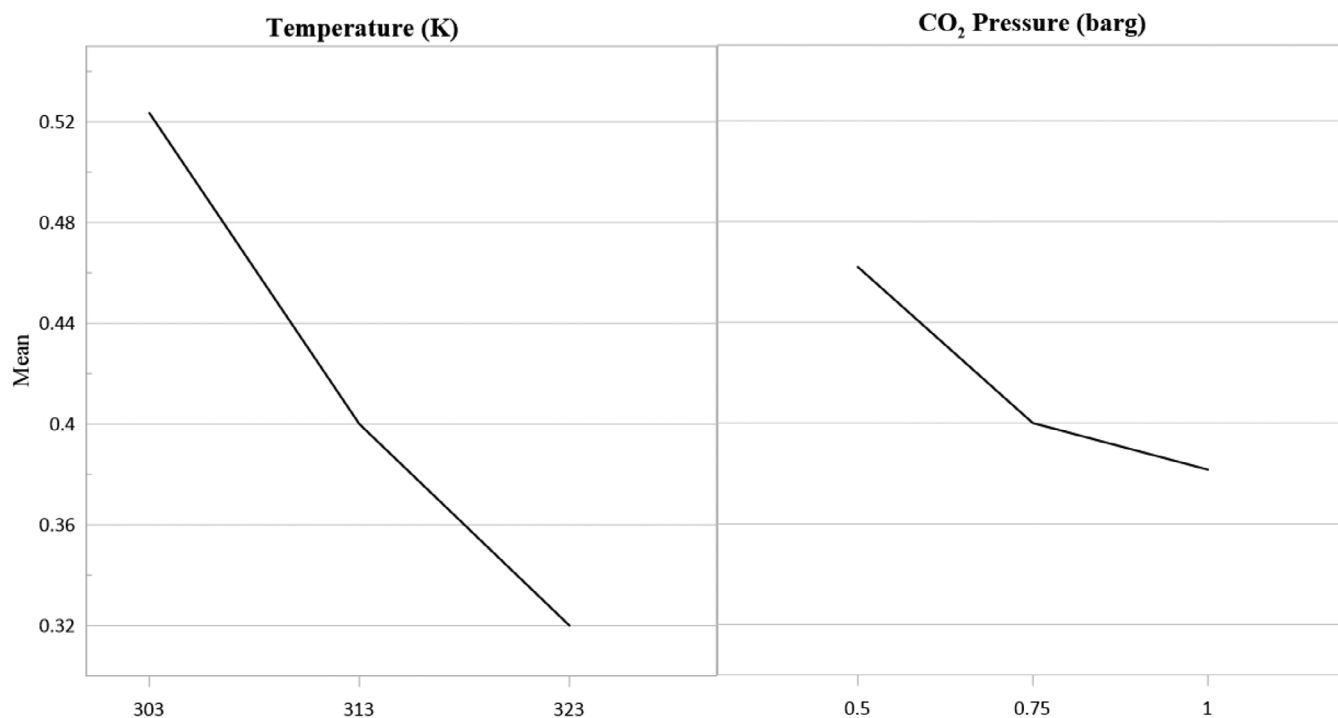
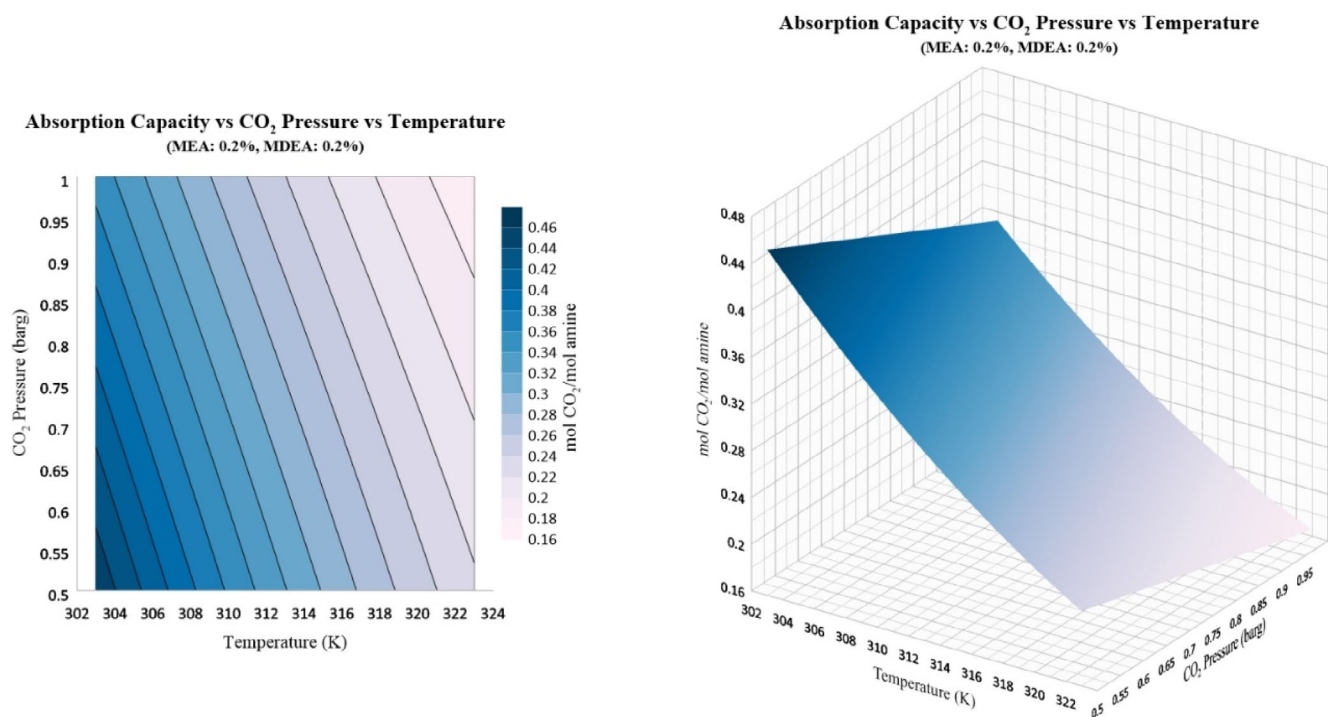**FIGURE 6** Main effect plots for the absorption capacity

FIGURE 7 Contour (left) and response surface (right) plots for the absorption capacity at equal concentrations of MEA and MDEA (other concentrations can be found in the Supporting Information S3). MDEA, methyl diethanolamine; MEA, monoethanolamine

Second, the two levels of the process condition would limit the extent of optimization, which is also affected by the first reason (initial setting). Noteworthy, when the initial settings were set to 0.4/0.0 MEA/MDEA and 303 K/0.5 barg, the optimum reaction rate was 3.13e-5 kmol/m^2·s at 0.343/0.057 MEA/MDEA and
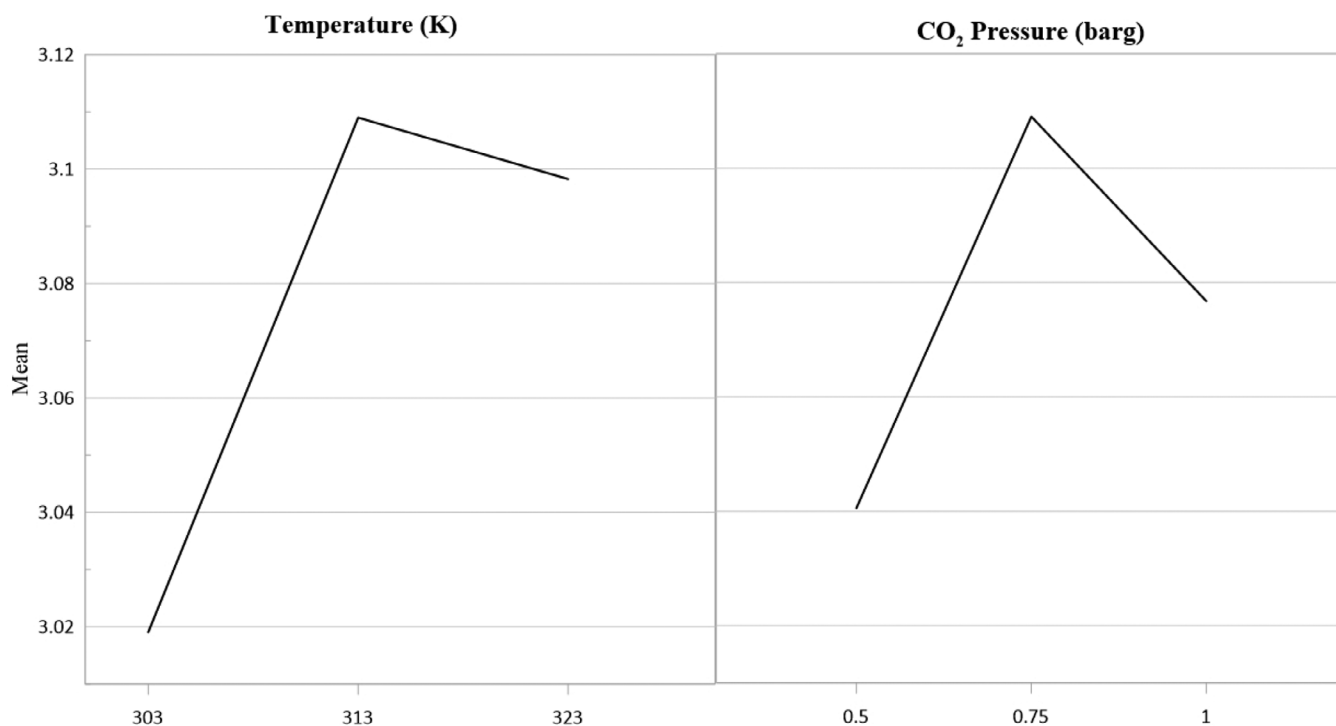
—WILEY⌐

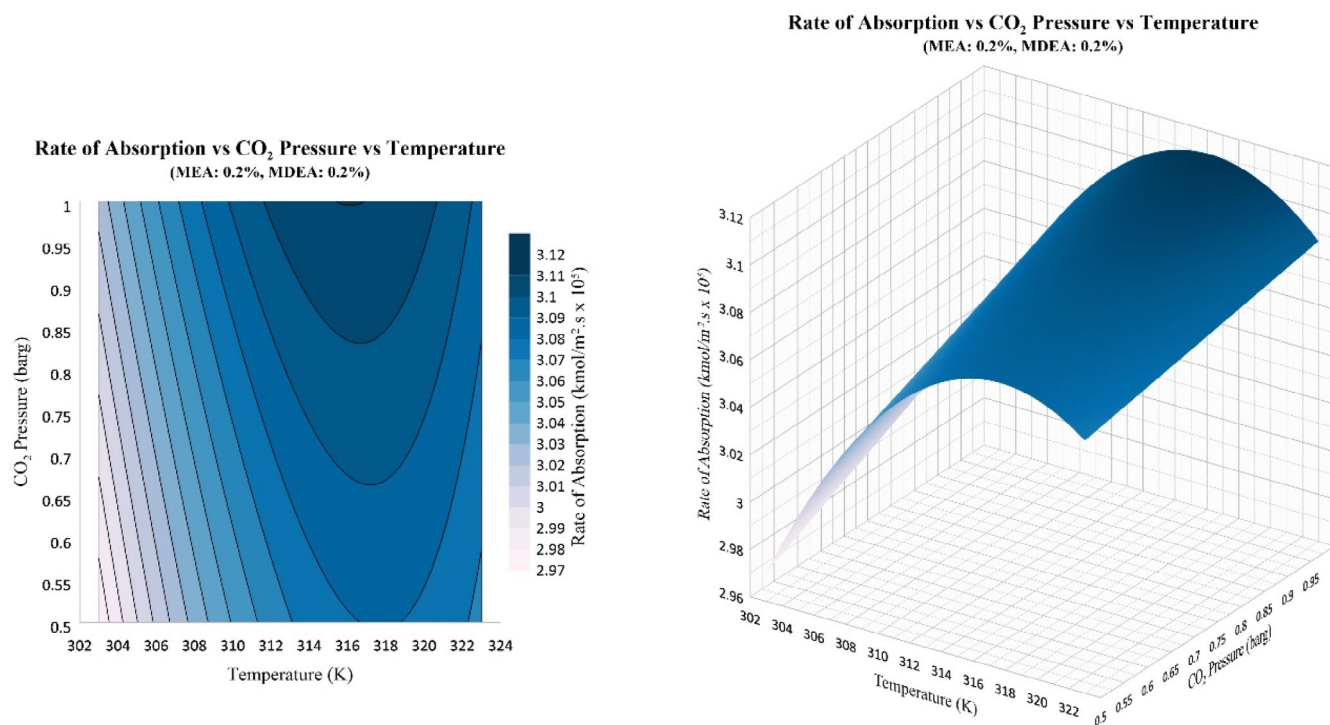**FIGURE 8**   Main effect plots for the reaction rate

FIGURE 9   Contour (left) and response surface (right) plots for the reaction rate at equal concentrations of MEA and MDEA (other concentrations can be found in the Supporting Information S3). MDEA, methyl diethanolamine; MEA, monoethanolamine

303 K/0.5 barg. On the contrary, the RSM optimization yielded the same results regardless of the initial settings. This shows the importance of considering more than two

levels for process conditions. The single-response optimization for both the absorption capacity and the reaction rate is shown in Figure 10.

TABLE 3 Confirmatory experiments with predicted responses using the mixture-process design models

No.	MEA (conc. %)	MDEA (conc. %)	Temperature (K)	CO_2 pressure (barg)	CO_2 loading (mol_{CO_2}/mol_{amine})	Predicted CO_2 loading (mol_{CO_2}/mol_{amine})	Rate of absorption (kmol/ $m^2 \cdot s$) $\times$ (10^5)	Predicted rate of absorption (kmol/ $m^2 \cdot s$) $\times$ (10^5)
51	20	20	308	0.6	0.49	0.46	3.098	3.076
52	20	20	308	0.9	0.46	0.42	3.102	3.083
53	20	20	318	0.6	0.31	0.35	3.093	3.065
54	20	20	318	0.9	0.45	0.31	3.105	3.072

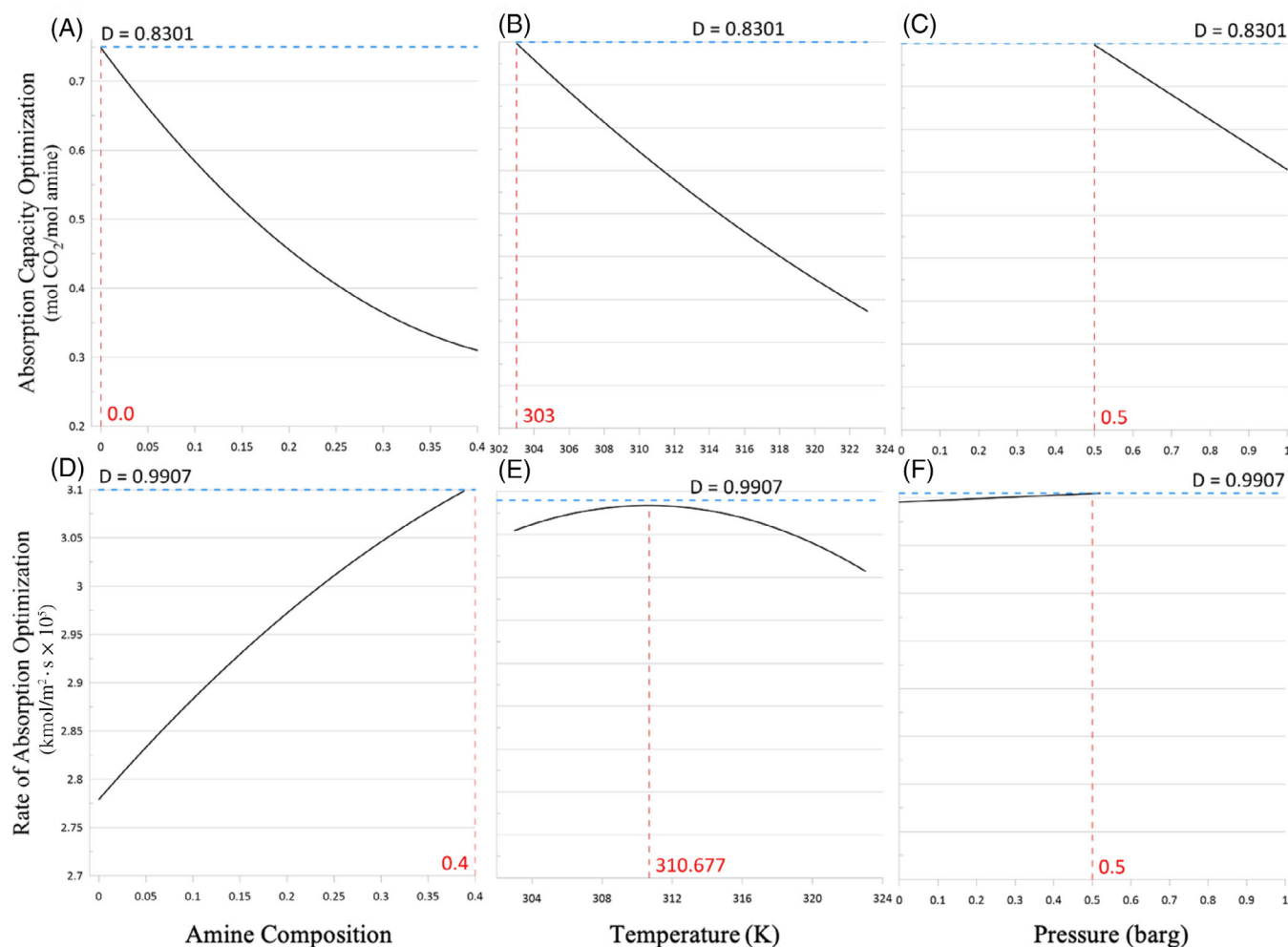Abbreviations: MDEA, methyl diethanolamine; MEA, monoethanolamine.

FIGURE 10 Single-response optimization for the absorption capacity and reaction rate. Plots A-C show the capacity vs amine composition, temperature, and pressure, respectively. Plots D-F show the same but for the rate of absorption

4.5 | Multiresponse optimization

Given the opposing trends of both responses, the composite desirability was needed to quantify the optimization quality. Table 4 presents the results for the multiresponse

optimization for different initial settings using the RSM models. Giving both responses the same weight (1:1 importance) yields a single answer regardless of the initial settings, which is a capacity of 0.653 mol_{CO_2}/mol_{amine}) and a reaction rate of 2.987e-5 kmol/$m^2 \cdot s$ at 0.0/0.4

TABLE 4 Multiresponse optimization results at different initial settings

Initial Settings			Importance	Multiresponse optimization results					
MEA (ratio)	Temperature (K)	Pressure (barg)	Capacity/rate	MEA (ratio)	Temperature (K)	Pressure (barg)	Capacity (mol_{CO_2}/mol_{amine})	Rate (kmol/$m^2 \cdot s \times 10^5$)	Desirability
0	303	0.5	1/1	0	313.3	0.5	0.653	2.987	0.903
0.4	303	0.5	1/1	0	313.3	0.5	0.653	2.987	0.903
0	313	0.75	1/1	0	313.3	0.5	0.653	2.987	0.903
0.4	313	0.75	1/1	0	313.3	0.5	0.653	2.987	0.903
0	323	1	1/1	0	313.3	0.5	0.653	2.987	0.903
0.4	323	1	1/1	0	313.3	0.5	0.653	2.987	0.903
0	303	0.5	1/2	0.0848	310.47	0.525	0.563	3.02	0.893
0.4	303	0.5	1/2	0.214	303	0.5	0.523	3.019	0.856
0	313	0.75	1/2	0	313	0.737	0.6	3.02	0.923
0.4	313	0.75	1/2 (1/1.6)	0.214	303	0.5	0.523	3.019	0.856 (0.837)
0	323	1	1/2	0	316.7	0.5	0.603	3.02	0.926
0.4	323	1	1/2	0.214	303	0.5	0.523	3.019	0.856
0	313	0.75	1/4	0	313	0.73	0.6	3.021	0.953
0.4	313	0.75	1/4	0.218	303	0.5	0.519	3.022	0.91
0	313	0.75	1/8	0	313	0.73	0.6	3.021	0.973
0.4	313	0.75	1/8	0.218	303	0.5	0.519	3.022	0.949

Note: The target for the absorption capacity and reaction rate is set as 0.705 mol_{CO_2}/mol_{amine} and 3.021e-5 kmol/$m^2 \cdot s$, respectively, while the minimum limit is set as the lowest value obtained across all data points. The results for the 1/1.6 ratio are essentially the same as 1/2 ratio just with lower desirability. An example is given for one case below (with initial settings 0.4, 313, 0.75, and 1/2).
Abbreviation: MEA, monoethanolamine.

MEA/MDEA and 313.3 K/0.5 barg. This indicates that the rate of change of the capacity with respect to the different factors is greater than that of the reaction rate. Hence, it would be desired to know at what importance the reaction rate moves the optimal point away from the 0.0 MEA concentration. With 1:2 (capacity to rate) importance, all initial settings have led to the target reaction rate (~ 3.02e-5 kmol/m^2·s), while the absorption capacity varied, yet more pronounced with the variation of MEA's concentration than with the process variables. For example, all cases with 0.4 MEA initial settings resulted in the same values regardless of the temperature and pressure ($D = 0.856$ for all cases). This signifies the dominant effect of the mixture composition over process conditions. Yet, at 0.0 MEA initial setting, different process variables settings resulted in different composite desirability values scoring 0.893, 0.923, and 0.926 for low, medium, and high levels of process variables, respectively. Such behavior can be attributed to the different trends of reaction rate at different process variables settings in Figure 5. Unlike the capacity, starting at a different set of process conditions would place the initial point of optimization at a different topology of the surface for the reaction rate, and by giving greater importance to the reaction rate over the capacity, the response optimizer would lean toward meeting the rate's target. As such, the rate seemed to reach the target value by slightly manipulating the process variables and by hardly changing MEA's composition (only in the low process variable initial setting). Increasing the importance of the reaction rate to 4 and 8 seems to yield a unified result, which is aligned with the 1:2 results. Although those optimization runs at 1:4 and 1:8 yielded higher composite desirability, it should be noted that such comparison is not valid as the powers in Equation (6) are different from other cases. Hence, only the cases of the same importance can be compared. Yet, it would be desired to know at which importance ratio the reaction rate starts to be considered. This ratio is henceforth called the critical importance ratio, which reveals at which level of importance does a response change comparably to the other response when a factor is changed. By trial-and-error methodology, it appeared that 1:1.6 (rate capacity) importance ratio is the critical value, in which different initial settings would yield multiple optimal responses. If considering more responses, possibly more solvent properties, one could quantify their dependence on process condition and mixture composition, allowing for rapid tuning of a solvent blend with certain targets (possibly dictated by some process constraints). Also, such a critical ratio can be used to obtain a quantitative feel of the extent by which responses would change, especially if coupled with monetary figures as in Mota-Martinez et al.[75]

5 | CONCLUSION

This study investigated a novel nonaqueous hexanol-based MEA/MDEA solvent for CO_2 capture by assessing the absorption capacity and reaction rate. Using a mixture-process design with a fixed amine concentration of 40%, five different ratios of MEA to MDEA were tested at four different temperature and pressure settings (40 experiments including replicas). The experiments were carried out in a jacketed stirred cell reactor with CO_2 pressure and temperature limits 0.5 to 1 barg and 303 to 323 K, respectively. A mathematical model was obtained using the mixture-process design for each response. The absorption capacity was observed to increase with higher MDEA concentration and lower temperature/pressure. On the contrary, the interaction of process variables at different amine concentrations seemed to have a more pronounced effect on the reaction rate, in which temperature was found to change the response topology. At low temperature, the response trace graph of the reaction rate exhibited a minimum and vice versa. This exemplifies the effect of temperature on the mixture formulation. To assess the effect of process variables more closely, five additional experiments (replicated once) were carried out at the center point of the process conditions (0.75 barg and 313 K). These additional points were modeled with the initial points and optimized using RSM. For single-response optimization, an optimum capacity of 0.83 was predicted at 0.0/0.4 MEA/MDEA and 303 K/0.5 barg conditions, while the optimum reaction rate was found 3.17e-5 kmol/m^2·s at 0.4/0.0 MEA/MDEA and 310.67 K/0.5 barg. Multiresponse optimization was carried out using the composite desirability function at different initial settings and importance ratios. With equal importance for the capacity and reaction rate, the optimization leads to a single optimum regardless of the initial settings (0.653 mol$_{CO_2}$/mol$_{amine}$ and 2.987e-5 kmol/m^2·s at 0.0/0.4 MEA/MDEA and 313.3 K/0.5 barg with $D = 0.903$). Increasing the importance of the reaction rate above 1.6 yields multiple optima, especially when starting at 0.0/0.4 MEA/MDEA setting.

Exploring new solvent formulations using statistical methods such as mixture-process design and RSM is cost-effective in evaluating multiple responses simultaneously and optimizing the composition of mixtures. Finding the relative importance in the multiresponse optimization can aid in assessing the extent of the solvent's performance at a process condition, and whether it is possible to achieve desired values, especially for responses with no mutual optima.

CONFLICT OF INTEREST

The authors declare no potential conflict of interest.

DATA AVAILABILITY STATEMENT

The authors confirm that the data supporting the findings of this study are available within the article [and/or] its supplementary materials.

ORCID

Neslisah Ulus https://orcid.org/0000-0002-5348-0314
Shafeeq Ahmed Syed Ali https://orcid.org/0000-0002-2642-216X
Omar Khalifa https://orcid.org/0000-0002-7710-5113
Ozge Yuksel Orhan https://orcid.org/0000-0003-0135-0363
Ali Elkamel https://orcid.org/0000-0002-6220-6288

REFERENCES

1. Songolzadeh M, Soleimani M, Takht Ravanchi M, Songolzadeh R. Carbon dioxide separation from flue gases: a technological review emphasizing reduction in greenhouse gas emissions. *Sci World J*. 2014;2014:828131.
2. IPCC, Edenhofer O, Pichs-Madruga R, Sokona Y, et al. Summary for policy-makers. *Climate Change 2014: Mitigation of Climate Change. Contribution of Working Group III to the Fifth Assessment Report of the Intergovernmental Panel on Climate Change*. Cambridge England: Cambridge University Press; 2014.
3. Plaza MG, Pevida C. Current status of CO_2 capture from coal facilities. In: Suárez-Ruiz I, Diez MA, Rubiera F, eds. *New Trends in Coal Conversion*. Sawston, England: Woodhead Publishing; 2019:31-58.
4. Subraveti SG, Pai KN, Rajagopalan AK, et al. Cycle design and optimization of pressure swing adsorption cycles for pre-combustion CO_2 capture. *Appl Energy*. 2019;254:113624.
5. Wu H-B, Xu M-X, Li Y-B, Wu J-H, Shen J-C, Liao H. Experimental research on the process of compression and purification of CO_2 in oxy-fuel combustion. *Applied Energy*. 2020;259:114123.
6. Vega F, Camino S, Camino JA, Garrido J, Navarrete B. Partial oxy-combustion technology for energy efficient CO_2 capture process. *Appl Energy*. 2019;253:113519.
7. Wu X, Wang M, Liao P, Shen J, Li Y. Solvent-based post-combustion CO_2 capture for power plants: a critical review and perspective on dynamic modelling, system identification, process control and flexible operation. *Appl Energy*. 2020;257:113941.
8. Vega F, Cano M, Camino S, Gallego Fernández LM, Portillo E, Navarrete B. Solvents for carbon dioxide capture. In: Karamé I, Shaya J, Hassan S, eds. *Carbon Dioxide Chemistry, Capture and Oil Recovery*. London, England: IntechOpen; 2018.
9. Li B-H, Zhang N, Smith R. Simulation and analysis of CO_2 capture process with aqueous monoethanolamine solution. *Appl Energy*. 2016;161:707-717.
10. Plaza MG, Rubiera F. Evaluation of a novel multibed heat-integrated vacuum and temperature swing adsorption post-combustion CO_2 capture process. *Appl Energy*. 2019;250:916-925.
11. Jiang L, Gonzalez-Diaz A, Ling-Chin J, Roskilly AP, Smallbone AJ. Post-combustion CO_2 capture from a natural gas combined cycle power plant using activated carbon adsorption. *Appl Energy*. 2019;245:1-15.
12. Lee S, Yun S, Kim J-K. Development of novel sub-ambient membrane systems for energy-efficient post-combustion CO_2 capture. *Appl Energy*. 2019;238:1060-1073.
13. Daneshvar E, Wicker RJ, Show PL, Bhatnagar A. Biologically-mediated carbon capture and utilization by microalgae towards sustainable CO_2 biofixation and biomass valorization—a review. *Chem Eng J*. 2022;427:130884.
14. Zanganeh KE, Shafeen A, Salvador C. CO_2 capture and development of an advanced pilot-scale cryogenic separation and compression unit. *Energy Procedia*. 2009;1(1):247-252.
15. Feron PHM, Cousins A, Jiang K, Zhai R, Garcia M. An update of the benchmark post-combustion CO_2-capture technology. *Fuel*. 2020;273:117776.
16. Oexmann J. *Post-Combustion CO_2 Capture: Energetic Evaluation of Chemical Absorption Processes in Coal-Fired Steam Power Plants*. Hamburg: University library of the TU Hamburg-Harburg; 2011.
17. Idem R, Wilson M, Tontiwachwuthikul P, et al. Pilot plant studies of the CO_2 capture performance of aqueous MEA and mixed MEA/MDEA solvents at the University of Regina CO_2 capture technology development plant and the boundary dam CO_2 capture demonstration plant. *Ind Eng Chem Res*. 2006;45(8):2414-2420.
18. Law LC, Yusoff Azudin N, Abd Shukor SR. Optimization and economic analysis of amine-based acid gas capture unit using monoethanolamine/methyl diethanolamine. *Clean Techn Environ Policy*. 2018;20(3):451-461.
19. Nuchitprasittichai A, Cremaschi S. Optimization of CO_2 capture process with aqueous amines—a comparison of two simulation–optimization approaches. *Ind Eng Chem Res*. 2013;52(30):10236-10243.
20. Kim YE, Park JH, Yun SH, Nam SC, Jeong SK, Yoon YI. Carbon dioxide absorption using a phase transitional alkanolamine–alcohol mixture. *J Ind Eng Chem*. 2014;20(4):1486-1492.
21. Vitillo JG. Introduction: carbon capture and separation. *Chem Rev*. 2017;117(14):9521-9523.
22. Lloret JO, Vega LF, Llovell F. A consistent and transferable thermodynamic model to accurately describe CO_2 capture with monoethanolamine. *J CO2 Util*. 2017;21:521-533.
23. Goto K, Yogo K, Higashii T. A review of efficiency penalty in a coal-fired power plant with post-combustion CO_2 capture. *Appl Energy*. 2013;111:710-720.
24. Khalifa O, Alkhatib III, Bahamon D, Alhajaj A, Abu-Zahra MRM, Vega LF. Modifying absorption process configurations to improve their performance for post-combustion CO_2 capture—what have we learned and what is still missing? *Chem Eng J*. 2022;430:133096.
25. Heldebrant DJ, Koech PK, Glezakou VA, Rousseau R, Malhotra D, Cantu DC. Water-lean solvents for post-combustion CO_2 capture: fundamentals, uncertainties, opportunities, and outlook. *Chem Rev*. 2017;117(14):9594-9624.

26. Henni A, Mather AE. Solubility of carbon dioxide in methyl-diethanolamine + methanol + water. *J Chem Eng Data*. 1995; 40(2):493-495.

27. Oyevaar MH, Fontein HJ, Westerterp KR. Equilibria of carbon dioxide in solutions of diethanolamine in aqueous ethylene glycol at 298 K. *J Chem Eng Data*. 1989;34(4):405-408.

28. Wanderley RR, Ponce GJC, Knuutila HK. Solubility and heat of absorption of CO_2 into diisopropylamine and *N,N*-diethylethanolamine mixed with organic solvents. *Energy Fuels*. 2020;34(7):8552-8561.

29. Hwang J, Kim J, Lee HW, et al. An experimental based optimization of a novel water lean amine solvent for post combustion CO_2 capture process. *Appl Energy*. 2019;248:174-184.

30. Guo H, Li C, Shi X, Li H, Shen S. Nonaqueous amine-based absorbents for energy efficient CO_2 capture. *Appl Energy*. 2019; 239:725-734.

31. Wang R, Liu S, Wang L, et al. Superior energy-saving splitter in monoethanolamine-based biphasic solvents for CO_2 capture from coal-fired flue gas. *Appl Energy*. 2019;242:302-310.

32. Zhang S, Shen Y, Wang L, Chen J, Lu Y. Phase change solvents for post-combustion CO_2 capture: principle, advances, and challenges. *Appl Energy*. 2019;239:876-897.

33. Li C, Shi X, Shen S. Performance evaluation of newly developed absorbents for solvent-based carbon dioxide capture. *Energy Fuels*. 2019;33(9):9032-9039.

34. Montgomery DC. *Design and Analysis of Experiments*. 8th ed. New York, NY: John Wiley & Sons, Inc.; 2017.

35. Cornell JA. Experiments with mixtures: a review. *Dent Tech*. 1973;15(3):437-455.

36. Cornell JA. *Experiments with Mixtures: Designs, Models, and the Analysis of Mixture Data*. 3rd edn. New York: John Wiley & Sons, Inc; 2002.

37. Cornell JA, ed. The inclusion of process variables in mixture experiments. *Experiments With Mixtures: Designs, Models, and the Analysis of Mixture Data*. New York: John Wiley & Sons, Inc; 2002:354-437.

38. Jahan A, Edwards KL, Bahraminasab M. 6—Multiple objective decision-making for material and geometry design. In: Jahan A, Edwards KL, Bahraminasab M, eds. *Multi-Criteria Decision Analysis for Supporting the Selection of Engineering Materials in Product Design*. 2nd ed. Oxford, England: Butterworth-Heinemann; 2016:127-146.

39. Hemmati A, Rashidi H. Optimization of industrial intercooled post-combustion CO_2 absorber by applying rate-base model and response surface methodology (RSM). *Process Saf Environ Prot*. 2019;121:77-86.

40. Song C, Kitamura Y, Li S. Optimization of a novel cryogenic CO_2 capture process by response surface methodology (RSM). *J Taiwan Inst Chem Eng*. 2014;45(4):1666-1676.

41. Neethu B, Tholia V, Ghangrekar MM. Optimizing performance of a microbial carbon-capture cell using Box-Behnken design. *Process Biochem*. 2020;95:99-107.

42. Pashaei H, Ghaemi A, Nasiri M, Karami B. Experimental modeling and optimization of CO_2 absorption into piperazine solutions using RSM-CCD methodology. *ACS Omega*. 2020; 5(15):8432-8448.

43. Setameteekul A, Aroonwilas A, Veawab A. Statistical factorial design analysis for parametric interaction and empirical correlations of CO_2 absorption performance in MEA and blended MEA/MDEA processes. *Sep Purif Technol*. 2008;64(1): 16-25.

44. Zainul Anuar MAU, Taha MF, Md Yunus NM, Mat Ghani SM, Idris A. An optimization study of carbon dioxide absorption into the aqueous solution of monoethanolamine and tetrabutylphosphonium methanesulfonate hybrid solvent using RSM-CCD methodology. *Processes*. 2021;9(7).1186.

45. Allahyarzadeh-Bidgoli A, Hamidishad N, Yanagihara JI. Carbon capture and storage energy consumption and performance optimization using metamodels and response surface methodology. *J Energy Resour Technol*. 2021;144(5):050901.

46. Caplow M. Kinetics of carbamate formation and breakdown. *J Am Chem Soc*. 1968;90(24):6795-6803.

47. da Silva EF, Svendsen HF. Ab initio study of the reaction of carbamate formation from CO_2 and alkanolamines. *Ind Eng Chem Res*. 2004;43(13):3413-3418.

48. Crooks JE, Donnellan JP. Kinetics and mechanism of the reaction between carbon-dioxide and amines in aqueous solution. *J Chem Soc-Perkin Trans 2*. 1989;4:331-333.

49. Littel RJ, Versteeg GF, Vanswaaij WPM. Kinetics of CO_2 with primary and secondary-amines in aqueous solutions—I. Zwitterion deprotonation kinetics for DEA and DIPA in aqueous blends of alkanolamines. *Chem Eng Sci*. 1992;47(8): 2027-2035.

50. Vaidya P, Kenig E. CO_2-alkanolamine reaction kinetics: a review of recent studies. *Chem Eng Technol*. 2007;30:1467-1474.

51. Vaidya P, Kenig E. Termolecular kinetic model for CO_2-alkanolamine reactions: an overview. *Chem Eng Technol*. 2010; 33:1577-1581.

52. Thee H, Nicholas NJ, Smith KH, da Silva G, Kentish SE, Stevens GW. A kinetic study of CO_2 capture with potassium carbonate solutions promoted with various amino acids: glycine, sarcosine and proline. *Int J Greenh Gas Control*. 2014;20: 212-222.

53. Thee H, Suryaputradinata YA, Mumford KA, et al. A kinetic and process modeling study of CO_2 capture with MEA-promoted potassium carbonate solutions. *Chem Eng J*. 2012; 210:271-279.

54. Orhan OY, Alper E. Kinetics of reaction between CO_2 and ionic liquid-carbon dioxide binding organic liquid hybrid systems: analysis of gas-liquid absorption and stopped flow experiments. *Chem Eng Sci*. 2017;170:36-47.

55. Cihan N, Orhan OY, Ersan HY. Effect of non-aqueous solvents on kinetics of carbon dioxide absorption by $^{t}Bu_3P/B(C_6F_5)_3$ frustrated Lewis pairs. *Sep Purif Technol*. 2021;258:7.

56. Yuksel Orhan O. Effects of various anions and cations in ionic liquids on CO_2 capture. *J Mol Liq*. 2021;333:115981.

57. Orhan OY. Investigation of biocatalytic absorption and ultrasound-assisted desorption performance of CO_2 capture. *Hacet J Biol Chem*. 2021;49(1):57-68.

58. Croarkin C, Tobias P. *NIST/SEMATECH e-Handbook of Statistical Methods*. USA: NIST/SEMATECH; 2006. http://www.itl.nist.gov/div898/handbook (accessed Feb 1, 2022).

59. Barzagli F, Giorgi C, Mani F, Peruzzini M. Reversible carbon dioxide capture by aqueous and non-aqueous amine-based absorbents: a comparative analysis carried out by ^{13}C NMR spectroscopy. *Appl Energy*. 2018;220:208-219.

60. El Hadri N, Quang DV, Goetheer ELV, Abu Zahra MRM. Aqueous amine solution characterization for post-combustion CO_2 capture process. *Appl Energy*. 2017;185: 1433-1449.

61. Chowdhury FA, Okabe H, Yamada H, Onoda M, Fujioka Y. Synthesis and selection of hindered new amine absorbents for CO_2 capture. *Energy Procedia*. 2011;4:201-208.

62. Dang HY, Rochelle G. CO_2 absorption rate and solubility in monoethanolamine/piperazine/water. *Sep Sci Technol*. 2003; 38:337-357.

63. Zhang R, Zhang X, Yang Q, Yu H, Liang Z, Luo X. Analysis of the reduction of energy cost by using MEA-MDEA-PZ solvent for post-combustion carbon dioxide capture (PCC). *Appl Energy*. 2017;205:1002-1011.

64. Choi W-J, Seo JB, Jang SY, Jung JH, Oh KJ. Removal characteristics of CO_2 using aqueous MEA/AMP solutions in the absorption and regeneration process. *J Environ Sci*. 2009;21(7): 907-913.

65. Bougie F, Pokras D, Fan X. Novel non-aqueous MEA solutions for CO_2 capture. *Int J Greenh Gas Control*. 2019;86: 34-42.

66. Porcheron F, Gibert A, Mougin P, Wender A. High throughput screening of CO_2 solubility in aqueous monoamine solutions. *Environ Sci Technol*. 2011;45(6):2486-2492.

67. Chen S, Chen S, Zhang Y, Qin L, Guo C, Chen J. Species distribution of CO_2 absorption/desorption in aqueous and non-aqueous *N*-ethylmonoethanolamine solutions. *Int J Greenh Gas Control*. 2016;47:151-158.

68. Mahmoodi R, Mofarahi M, Izadpanah AA, Afkhamipour M, Hajizadeh A. Experimental and theoretical investigation of equilibrium absorption performance: effect of alkyl amines as promoters on the CO_2 loading of 2-amino-2-methyl-1-propanol at 313 K. *Energy Fuels*. 2019;33(9):8985-8997.

69. Barzagli F, Mani F, Peruzzini M. Efficient CO_2 absorption and low temperature desorption with non-aqueous solvents based on 2-amino-2-methyl-1-propanol (AMP). *Int J Greenh Gas Control*. 2013;16:217-223.

70. Lin P-H, Wong DSH. Carbon dioxide capture and regeneration with amine/alcohol/water blends. *Int J Greenh Gas Control*. 2014;26:69-75.

71. Hamidi R, Farsi M, Eslamloueyan R. CO_2 solubility in aqueous mixture of MEA, MDEA and DAMP: absorption capacity, rate and regeneration. *J Mol Liq*. 2018;265:711-716.

72. Sema T, Naami A, Liang Z, Idem R, Ibrahim H, Tontiwachwuthikul P. 1D absorption kinetics modeling of CO_2–DEAB–H_2O system. *Int J Greenh Gas Control*. 2013;12: 390-398.

73. Brea U, Gómez-Díaz D, Navaza JM, Rumbo A. Carbon dioxide chemical absorption in non-aqueous solvents by the presence of water. *J Taiwan Inst Chem Eng*. 2019;102:250-258.

74. Wilcox J, ed. Absorption. *Carbon Capture*. New York, NY: Springer; 2012:53-113.

75. Mota-Martinez MT, Hallett JP, Mac Dowell N. Solvent selection and design for CO_2 capture—how we might have been missing the point. *Sustain Energy Fuels*. 2017;1(10):2078-2090.

SUPPORTING INFORMATION

Additional supporting information may be found in the online version of the article at the publisher's website.